PROCEEDINGS OF SCIENCE

Finite difference method calculations of three-particle energy spectra

P. Danev,* H. Tonchev, Zh. Stoyanov, Y. Mutafchieva and M. Stoilov

Institute for Nuclear Research and Nuclear Energy - Bulgarian Academy of Sciences, 72 Tzarigradsko Chaussée, Sofia, Bulgaria

E-mail: petar_danev@abv.bg

The high-precision spectroscopy of light atomic and molecular systems opens up the possibility for a more in-depth study of fundamental physical constants and the laws of nature. This is achieved by a juxtaposition of the data from modern experiments and accurate theoretical calculations. In this work, we show our results of precise computations of electronic and nonrelativistic energy spectra of three-particle systems. We are particularly interested in the cases of H_2^+ and $\bar{p}He^+$ which are presented in detail. In our approach, the electronic wavefunctions are computed by a two-dimensional finite difference method in prolate spheroidal coordinates. Uniformly and exponentially spaced grids with a varying number of nodes were used in the Schrödinger equation's discretization. Accurate molecular quadrupole moments for the studied systems are calculated with the obtained wavefunctions.

11th International Conference of the Balkan Physical Union (BPU11), 28 August - 1 September 2022 Belgrade, Serbia

*Speaker

PoS(BPU11)066

1. Introduction

The development of new experimental techniques, like trapping a small number of atoms or ions and cooling them to extremely low temperatures, leads to very accurate measurements of their energy and transition spectra [1–3]. The variational and adiabatic methods allow for achieving a comparable accuracy of the theoretical computations for various quantum quantities [4, 5]. Energy and transition spectra have been numerically obtained for a number of tree-body quantum systems, like for example $\bar{p}\mathrm{He}^+$ [6], D_2^+ [7] and muonic molecular ions [8]. By comparing the results from both experimental and theoretical studies of atomic systems, new knowledge about the laws of nature can be discovered and the values of fundamental constants can be obtained with a higher accuracy [2, 3, 9]. In particular, exotic atoms like antihydrogen and antiprotonic helium could also allow comparison between matter and antimatter characteristics and test the CPT symmetry [10].

In this work, we study three-particle atomic and molecular systems. Since they consist of only a few particles, their spectrum can be computed with high precision without making a lot of approximations [6, 11]. Their simplicity makes it possible to take into account the effects of much more subtle quantum electrodynamical corrections to their spectrum and therefore to investigate the nature of these effects. These light systems have such unique properties as long-lived metastable states and the existence of levels with low sensitivity to interactions with external fields [12]. Those characteristics introduce the possibility of using them in the development of new time standards, quantum gates and memories, etc. Here, we present accurate calculations of the electronic and nonrelativistic energy spectra of the three-particle systems H_2^+ and $\bar{p}\mathrm{He}^+$. In our approach, the electronic wavefunctions are computed by using a two-dimensional finite difference method. The electronic part of the Schrödinger equation is written in spheroidal coordinates. The eigenvalues and the corresponding wavefunctions for the ground and a few excited states are found with high precision. The code's performance for completing various computations of quantum system's characteristics is investigated. Its efficiency is compared with an open source quantum chemistry software package. The results of implementing our code with equally and exponentially spaced grids have been analyzed and compared with other computations of the energy spectra of light atomic systems. We show that the level of precision allows our results to be used in: computations of important spectroscopic quantities such as the molecular dipole and quadrupole moments, leading relativistic corrections to transition spectra of the studied systems and determining the effects of interactions with external fields. We have used the obtained electronic wavefunctions and terms in calculating the matrix elements of the molecular electric quadrupole moment and in solving the radial Schrödinger equation.

The paper is organized as follows. In Sec. 2, the Schrödinger equation in spheroidal coordinates for three-particle systems is presented. Sec. 3 provides an overview of the method used in the work. In Sec. 4 are presented the main results obtained with our code. The calculated electronic energies for H_2^+ and $\bar{p}\mathrm{He}^+$ are detailed in Subsec. 4.1. A comparison of the obtained precision depending on the different computational settings is also made there. In Subsec. 4.2, the molecular quadrupole moments of the antiprotonic helium and hydrogen molecular ions are calculated with the electronic wavefunctions. And in Subsec. 4.3 are presented the results from the computation of the nonrelativistic spectra of three-particle systems in the Born-Oppenheimer approximation. The concluding remarks are given in Sec. 5.

2. Three-particle systems

The nonrelativistic Hamiltonian of a three-particle system in atomic units ($e = \hbar = m_e = 1$) is:

$$H = \frac{\mathbf{p}_1^2}{2m_1} + \frac{\mathbf{p}_2^2}{2m_2} + \frac{\mathbf{p}_3^2}{2m_3} + \frac{Z_1 Z_3}{r_1} + \frac{Z_2 Z_3}{r_2} + \frac{Z_1 Z_2}{R}. \tag{1}$$

Here, $\mathbf{p}_i, m_i$, and $Z_i, i = 1, 2, 3$ are the momentum, mass, and charge of the particles and the distances between them are r_1, r_2, and $R = |\mathbf{r}_1 - \mathbf{r}_2|$ as shown on Fig. 1.

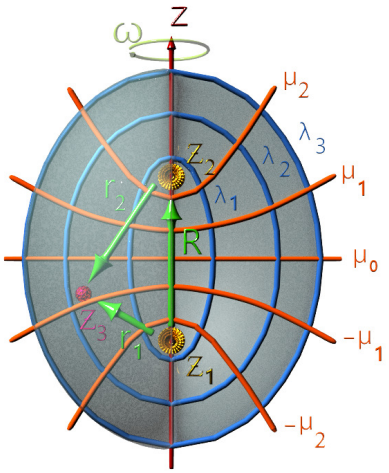

Figure 1: (Color online) A three-particle system in prolate spheroidal coordinates.

After separating the center-of-mass degrees of freedom, the total remaining wavefunction can be written as (see for example [5]):

$$\Psi_{m_J}^{\nu J}(\mathbf{r}, \mathbf{R}) = \sum_{m=0}^{J} \mathcal{D}_{mm_J}^{J}(\Phi, \Theta, \omega) F_m^{\nu J}(\mathbf{r}, R), \tag{2}$$

where $\mathcal{D}_{mm_J}^{J p_\lambda}(\Phi, \Theta, \omega)$ are the symmetrized Wigner functions. Here Φ, Θ, ω are the Euler angles of the vector $\mathbf{r}$ (the vector connecting the midpoint of R with the third particle) relative to the laboratory frame, while ν and J are the vibrational and total orbital momentum quantum numbers. The function $F_m^{\nu J p_\lambda}(\mathbf{r}, R)$ describes the system in a frame co-rotating with the plane containing the three particles. It can be factorized as:

$$F_m^{\nu J}(\mu, \lambda, R) = \sum_{n_\mu=0}^{\infty} \sum_{n_\lambda=0}^{\infty} \varphi^{m n_\mu n_\lambda}(R; \mu, \lambda) R^{-1} \chi_{\nu J}^{m n_\mu n_\lambda}(R). \tag{3}$$

The wavefunction $\chi_{\nu J}^{m n_\mu n_\lambda}(R)$ is the radial part of $F_m^{\nu J}$ expressed in spheroidal coordinates, as can be seen for example in Ref. [5], by using the following transformations (the coordinate frame is visualized on Fig. 1):

$$\begin{aligned} \lambda &= (r_1 + r_2)/R, \ 1 \le \lambda < \infty, \\ \mu &= (r_1 - r_2)/R, \ -1 \le \mu \le 1. \end{aligned} \tag{4}$$

The factorization of the three-particle nonrelativistic wavefunction is possible due to the separability of the total Hamiltonian given by Eq. (1). We study that part of the Hamiltonian describing the third and lightest particle in the Coulomb potential of two charges with infinite masses. By making the transformations shown above, the Hamiltonian can be written in prolate spheroidal coordinates. Detailed description of the procedure is illustrated in [5, 13], but will be briefly summarized below:

$$\tilde{H}^{sph} = \frac{-2}{MR^2(\lambda^2-\mu^2)}\left[\frac{\partial}{\partial\lambda}(\lambda^2-1)\frac{\partial}{\partial\lambda} + \frac{\partial}{\partial\mu}(1-\mu^2)\frac{\partial}{\partial\mu} - \frac{m^2(\lambda^2-\mu^2)}{(\lambda^2-1)(1-\mu^2)}\right] + \frac{2Z_1Z_3}{R(\lambda^2-\mu^2)}\left[\lambda\left(\frac{Z_2}{Z_1}+1\right)+\mu\left(\frac{Z_2}{Z_1}-1\right)\right], \tag{5}$$

where $M = m_3(m_1+m_2)/(m_1+m_2+m_3)$ is the reduced mass. If we substitute the units of the charge and mass ($e = -Z_1Z_3/2 = 1, m = 2M = 1$), as is done in Ref. [13], the resulting Hamiltonian will become quite general. In this case, it will depend only on the charge ratio $q = Z_2/Z_1$ and its eigenvalues will be in atomic units multiplied by the factor eM (i.e. $eM\times$ a.u. units of energy):

$$H^{sph} = \frac{-4}{R^2(\lambda^2-\mu^2)}\left[\frac{\partial}{\partial\lambda}(\lambda^2-1)\frac{\partial}{\partial\lambda} + \frac{\partial}{\partial\mu}(1-\mu^2)\frac{\partial}{\partial\mu} - \frac{m^2(\lambda^2-\mu^2)}{(\lambda^2-1)(1-\mu^2)} - 4R\left[\lambda\left(q+1\right)+\mu\left(q-1\right)\right]\right]. \tag{6}$$

By solving the Schrödinger equation for the electronic Hamiltonian

$$H^{sph}\varphi^{m\,n_\mu n_\lambda}(\mu,\lambda;R) = \varepsilon^{m\,n_\mu n_\lambda}\varphi^{m\,n_\mu n_\lambda}(\mu,\lambda;R), \tag{7}$$

we can find the electronic energies $\varepsilon^{m\,n_\mu n_\lambda}$ and the wavefunction $\varphi^{m\,n_\mu n_\lambda}(\mu,\lambda;R)$ defined in Eq. (3). The quantum numbers n_λ, and n_μ correspond to the number of plane crossings of $\varphi^{m\,n_\mu n_\lambda}(\mu,\lambda;R)$ in directions λ and μ, as visualized on Fig. 2. The remaining quantum number $m = 0, 1, 2, \ldots$ is the integer eigenvalue in the expression:

$$\frac{d^2\Omega^m(\omega)}{d\omega^2} + m^2\Omega^m(\omega) = 0, \quad 0 \le \omega \le 2\pi. \tag{8}$$

The total electronic wavefunction is given by

$$\phi^{m,n_\lambda,n_\mu}(\mu,\lambda;R,\omega) = \varphi^{m\,n_\mu n_\lambda}(\mu,\lambda;R)\Omega^m(\omega) = \varphi^{m\,n_\mu n_\lambda}(\mu,\lambda;R)e^{\pm im\omega}/\sqrt{2\pi}, \tag{9}$$

with normalization condition

$$\int_{-1}^{1}\int_{1}^{\infty}\int_{0}^{2\pi} dV\,|\phi^{m,n_\lambda,n_\mu}(\mu,\lambda;R,\omega)|^2 = 1, \qquad dV = \frac{R^3}{8}(\lambda^2-\mu^2)d\mu d\lambda d\omega. \tag{10}$$

We will note that for $m > 0$, there are numerical issues in the direct computation of the electronic wavefunctions, which leads to precision loss. To overcome it, the following substitution for $\varphi^{m\,n_\mu n_\lambda}(\mu,\lambda;R)$ is used in the numerical calculations:

$$\varphi^{m\,n_\mu n_\lambda}(\mu,\lambda;R) = (\lambda^2-1)^{m/2}(1-\mu^2)^{m/2}\tilde{\varphi}^{m\,n_\mu n_\lambda}(\mu,\lambda;R). \tag{11}$$

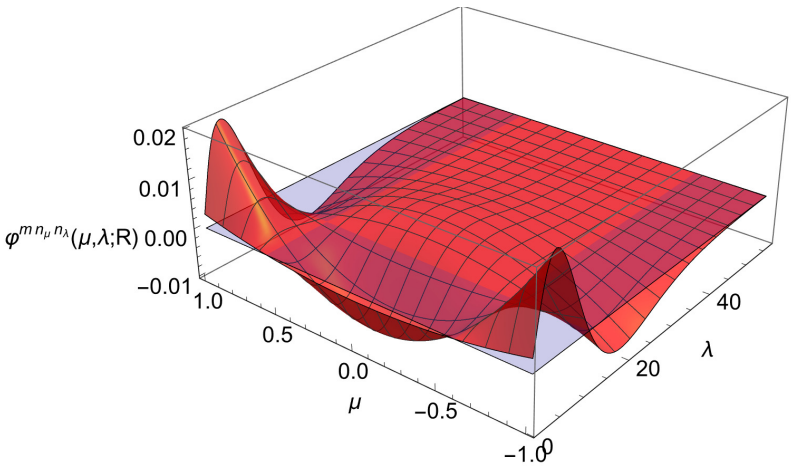

Figure 2: (Color online) Two-dimensional electronic wavefunction $\varphi^{m=0\,n_\mu=2\,n_\lambda=1}(\mu,\lambda;R)$ of H_2^+ with distance between the protons $R = 2$ a.u., obtained by 2D finite difference method. It can be seen that the section of the function along the μ coordinate axis crosses the plane two times, and so $n_\mu = 2$. While $n_\lambda = 1$ as the section of $\varphi^{0\,2\,1}(\mu,\lambda;R)$ along λ has one crossing.

3. Finite difference method on 2D non-equidistant grid

The eigenvalue problem (Eq. (7)) has been solved by a two-dimensional finite difference method [14]. We will review the procedure we have implemented and will show that it is simple to use and leads to high-precision results for the electronic wavefunctions and the electronic energies for a variety of problems similar to ours. Particular attention will be given to the type of the grid on which the Schrödinger equation is discretized, and we will show that using a non-equidistant one when other conditions are the same, increases the accuracy.

The eigenvalue problem for the electronic wavefunctions in spheroidal coordinates has been studied by many authors [5, 14, 15]. As the differential equation for $\varphi^{m\,n_\mu n_\lambda}(\mu,\lambda;R)$ is separable in the two variables λ and μ, usually in the literature both resulting equations are solvable in terms of a series expansion [15, 16]. A more straightforward method is adopted by Laaksonen [14], who solve the eigenvalue partial differential equation simultaneously for both variables. This is achieved by, first, a proper substitution of the variable λ, allowing for more precise computations. Then, a discretization of the Schrödinger equation in square grid points in the new variable and in μ is made, where a five- or seven-point stencil is used for the derivatives. Finally, a relaxation method is used to find the electronic energies. In contrast, our method consists of the following steps: discretization of the three-particle Hamiltonian, as given by Eq (7), on a 2D mesh of both μ and λ coordinates. A seven-point central stencil is used for all points, except for the ones close to the borders, where the stencil is calculated in such a way that no accuracy is lost. The second step is diagonalization of the Hamiltonian and finding the electronic wavefunctions and energies. They are represented by the Hamiltonian eigenvectors and eigenvalues respectively.

Here, a review of the finite difference method used on an exponential grid will be made, and in Sec. 4.1 we will show that a non-equidistant grid could significantly improve the precision of the calculations. Our method differs from the one described in Ref. [14] where the variables in the Schrödinger equation (7) are changed. For our approach, the grid points on which the discretization

is made could be modified in a way that it better corresponds to the behavior of the wavefunction. As in the case, where the radial part of the wavefunction changes fast for small λ (i.e. $\lambda \to 1$), increasing the grid point density at the beginning allows for our solution to better describe the actual wavefunction. Here, we will derive a general expression for stencil coefficients in the case of exponentially separated grid points. And we will use it to compute the electronic and nonrelativistic spectra of H_2^+ and $\bar{p}He^+$ that are presented in Sec. 4.

To simplify the presentation, we will investigate the case with a 1D grid. Higher dimension grids can be obtained by tensor multiplication of two or more 1D grids. Let us consider a mesh with k points, where each is in its node, and the j^{th} point is given by $x_j = \alpha^{h_j}$, $h_j = h_0 + j\Delta$, $j = 0 \div (k-1)$. Here, α is the base of the power law ($\alpha = 10$ in our computations), and Δ is the step, which is related to the total number of points N_x in the coordinate x. In turn, N_x depends on the required precision, the characteristics of the machine used for the calculations, etc. The N point stencil coefficients $a_i, i = 0, .., N-1$ for the grid point x_j are calculated by solving the system:

$$\begin{pmatrix} 1 & 1 & ... & 1 \\ \alpha^{p\Delta} - 1 & \alpha^{(p+1)\Delta} - 1 & ... & \alpha^{(p+N-1)\Delta} - 1 \\ ... & ... & ... & ... \\ (\alpha^{p\Delta} - 1)^{N-1} & (\alpha^{(p+1)\Delta} - 1)^{N-1} & ... & (\alpha^{(p+N-1)\Delta} - 1)^{N-1} \end{pmatrix} \begin{pmatrix} a_0 \\ a_1 \\ ... \\ a_{N-1} \end{pmatrix} = \frac{d!}{\alpha^{h_j}} \begin{pmatrix} \delta_{0d} \\ \delta_{1d} \\ ... \\ \delta_{N-1d} \end{pmatrix}$$

The parameter p in the above equation gives the position of the first stencil coefficient a_0 with respect to the j^{th} point on the grid. For example, to implement a five-point central exponential stencil, we have to set the following numerical values in the equation above: $N = 5$ and $p = -2$. In this case the d^{th} order derivative of the function $f(x_j)$ is $f(x_j)^{(d)} = \sum_{l=0}^{4} a_l f(x_{j-2+l})$.

By following this procedure for building a non-equidistant grid, a considerable improvement in the precision of the solution of Eq. (7) has been achieved. As it is quite general, it can be used when the finite difference method is applied to obtain more accurate results for a large class of eigenvalue problems.

For numerical calculations in atomic and molecular physics, there exist many program packages based on different theoretical methods. Variational computations are widely used due to the possibility for achieving high precision of the results [4, 6]. However, in some cases, they have long computational times and considerable resource requirements for calculations of a single atomic quantity. Moreover, often a comparison with calculations by different methods proves to be very helpful. Our code applies a finite difference method to compute the electronic spectrum of various three-particle systems by solving the Schrödinger equation in spheroidal coordinates. This has also been done by other authors, e.g. Refs. [5, 13–15]. However, the general approach to the problem is to use the separability of this particular equation and reduce it to a system of one-dimensional differential equations. In contrast, we solve the initial two-dimensional equation instead. This gives a few advantages, like the potential to: compute many electronic states simultaneously, add potentials to the Hamiltonian that are not separable, and apply the code to solve other general non-separable 2D differential equations. Additionally, the use of the presented code for computation of the electronic energies is quite straightforward - it does not require additional transformation of the differential equation or application of any other procedure, as done, for example, in the 2D finite difference code shown in Ref. [14].

Electronic energy ε^{000} of H_2^+ ground state at $R = 2$ a.u.			
Method	Total grid points	Electronic energy	Time, s
2D FD 7-point stencil	300	**−1.10263**44501691	< 1
2D FD 7-point stencil	1 200	**−1.1026342**359965	3.0
2D FD 7-point stencil	10 000	**−1.102634214**3509	23.2
2D FD 7-point stencil	40 000	**−1.102634214**4924	161.0
Hartree-Fock (Psi4)	—	**−1.10**0265	< 1
Electronic quadrupole moment of H_2^+ ground state at $R = 10$ a.u.			
		Electric quadrupole moment	Time, s
This work	—	**16.31635**100	< 1
Psi4	—	**16.**6148738	< 1
Nonrelativistic energy of H_2^+ ground state in the Born-Oppenheimer approximation			
Method	Total grid points	Nonrelativistic energy	Time, s
1D FD 3-point stencil	700	**−0.5971**02	< 1
1D FD 7-point stencil	900	**−0.5971**00	2.1
Psi4	—	**−0.60**026	< 1

Table 1: Performance of the presented code in computation of various tasks. The results from four calculations of the electronic energy of the ground electronic state $1s\sigma_g(000)$ of H_2^+ at internuclear distance $R = 2$ a.u. are given first. They are obtained by our two-dimensional finite difference method (2D FD) with an exponential grid and a seven-point stencil. In the second, third and fourth column are shown the total grid points used, the energy and the run-time. Next, the electronic quadrupole moment of the hydrogen molecular ion at $R = 10$ a.u. is presented. We will note that the values of the quadrupole moments differ from the ones in the next section by a factor 2/3 in order to match the definition from Ref. [17]. Finally, the nonrelativistic energy of the ground state of H_2^+ for two different configurations of our code using a one-dimensional finite difference method with 3- and 5-point stencils is shown. The reliable digits are in boldface and they are taken from Refs. [11, 14] and the references therein. Where possible, the performance is compared with computations by the quantum chemistry software package "Psi4" [17].

The performance of our code in various calculations is shown in Table 1. The electronic energy $\varepsilon^{m\,n_\lambda n_\mu}$ of H_2^+ ground electronic state $1s\sigma_g(m = 0\; n_\lambda = 0\; n_\mu = 0)$ at $R = 2$ a.u. is given in the beginning of the table. In all calculations, the 2D finite difference method with a seven-point stencil and an exponential grid is applied. The obtained results and the time needed to complete each run are presented for four different program configurations. The performance of our code to calculate the quadrupole moment and the nonrelativistic energy of H_2^+, are also shown in the table. To compute the latter quantities, the corresponding electronic wavefunctions have to be given as an input. To provide an independent basis for comparison, calculations similar to those above have been performed with the open-source python/c++ quantum chemistry software package "Psi4" [17] and these results are included in the table.

4. Numerical results

4.1 Three-particle electronic spectrum

By solving the Schrödinger equation Eq. (7) with the above-mentioned finite difference method for the spectra of one light particle in the Coulomb field of two particles with infinite mass, precise results for the energy values of the system can be obtained. We will show the results of two cases, that are of interest in spectroscopy. First, for a three-particle system with charges $Z_1 = 1, Z_2 = 1, Z_3 = -1$ - or as a particular case - for H_2^+-like systems. The second is for particles with $Z_1 = 2, Z_2 = -1, Z_3 = -1$, as is the antiprotonic helium. The electronic wavefunctions, the corresponding eigenvalues, and their derivatives in R, μ, and λ for those systems have been calculated for internuclear distances in the range $0 < R(a.u.) < R_{max}$, where R_{max} depends on the particular system and its state to be calculated.

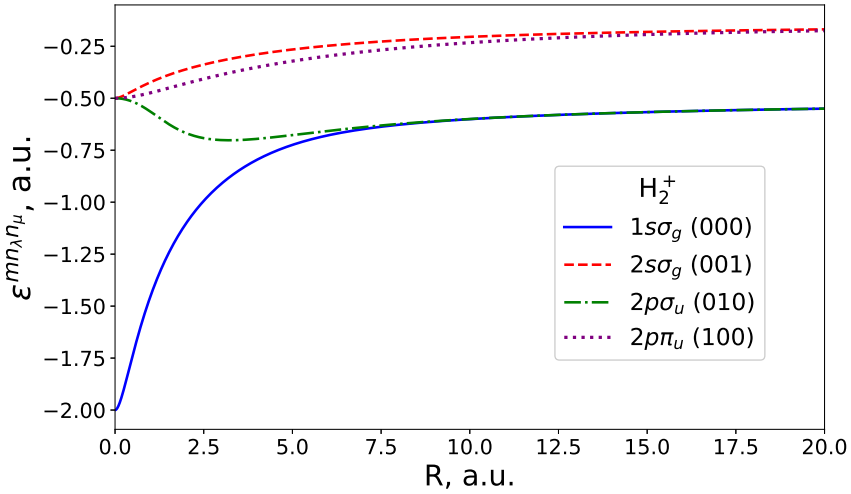

Figure 3: (Color online) The electronic energy curves $\varepsilon^{m\,n_\lambda n_\mu}(R)$ of H_2^+ like three-particle system for an internuclear distance up to $R = 20$ a.u. The ground $1s\sigma_g(000)$ and the three excited states $2s\sigma_g(001)$, $2p\sigma_u(010)$, and $1p\pi_u(100)$, are presented on the figure with solid blue, dashed red, dot-dashed green, and dotted purple lines respectively.

As an example, in the case of H_2^+, the energies $\varepsilon^{m\,n_\lambda n_\mu}$ of the four low-lying states: $1s\sigma_g(000)$, $2s\sigma_g(001)$, $2p\sigma_u(010)$, and $1p\pi_u(100)$, computed on an exponential grid for various values of the intermolecular distance R. The corresponding electronic energy curves are shown on Fig. 3. As for large internuclear distances, some of the electronic terms become indistinguishable since we have plotted them up to $R = 20$ a.u. Similarly, on Fig. 4 are shown the electronic terms for the $\bar{p}He^+$'s states: $1\sigma(000)$, $2\sigma(001)$, $3\sigma(010)$, and $1\pi(100)$.

More detailed information on the electronic energy calculations at internuclear distance $R = 2$ a.u. with both equally spaced and exponential grids and a comparison with results obtained by other methods [14, 15, 18] is given in Table 2. The presented results of the finite difference method's calculations with an equidistant grid have between five and ten correct digits (the boldface digits in the table are estimated by our code to be reliable), which shows that even the most direct approach

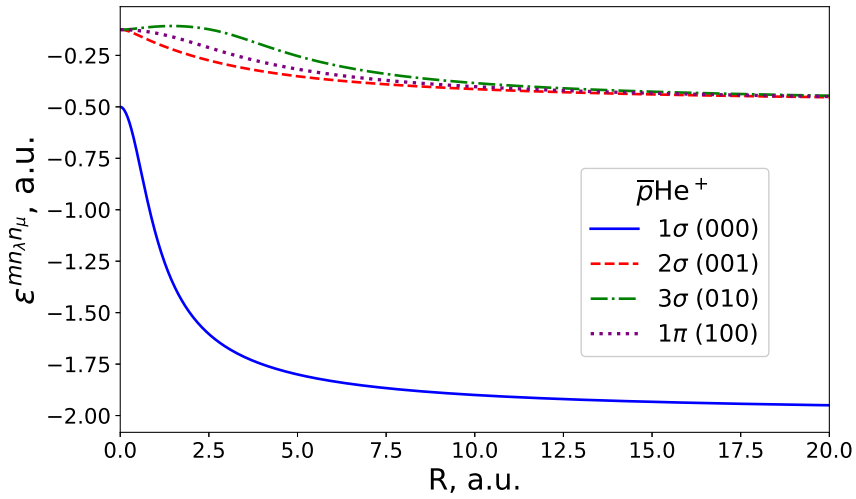

Figure 4: (Color online) The electronic energy curves $\varepsilon^{m\,n_\lambda n_\mu}(R)$ of $\bar{p}\mathrm{He}^+$ like three-particle system for an internuclear distance up to $R = 20$ a.u. The ground $1\sigma(000)$ and the three excited states $2\sigma(001)$, $3\sigma(010)$, and $1\pi(100)$, are presented on the figure with solid blue, dashed red, dot-dashed green, and dotted purple lines respectively.

to solving the eigenvalue problem, given by Eq. (7), is quite accurate in some cases. However, when an exponential grid is used in the discretization, the eigenvalues improve considerably and their precision becomes comparable with that of other accurate calculations of the electronic spectra of three-particle systems, as can be seen from Table 2. An equal number of points in μ and λ (N_μ and N_λ respectively) that depend on the particular system and state, are used in both the equidistant and exponential grids. The highest accuracy was achieved when $50 \leq N_\mu \leq 100$ and $200 \leq N_\lambda \leq 400$. We have presented the computed energy $\varepsilon^{m\,n_\lambda n_\mu}$ for the ground and a few low excited states, where the distance between the heavy particles is $R = 2$. The first column contains the quantum numbers of the electronic state. The naming convention commonly used in the literature (including in the cited references) is given first, and the ones defined by Eq. (3) are in brackets. The electronic energies of H_2^+ and $\bar{p}\mathrm{He}^+$-like systems in atomic units, calculated by the 2D finite difference method when equidistant and exponential grids (reviewed in Sec. 3) are used, are given in the second and third columns respectively. Similar results, obtained by other authors are shown in the last column(s) to compare the precision of our method. As can be seen from the table (more detailed explanations can be found for example in Ref. [15]), the accuracy of the electronic energies allows us to use the obtained wavefunctions in precision computations of Born-Oppenheimer and adiabatic nonrelativistic spectra, leading relativistic and spin contributions of the studied systems, and determining the effects of interactions with external fields.

4.2 Computation of H_2^+ and $\bar{p}\mathrm{He}^+$ quadrupole moments

The molecular electric multipole moments are important characteristics of the molecule as they give information on the charge distribution inside a molecule. Knowing their values with high precision allows us to obtain more accurate data on the molecule's structure, intermolecular forces, etc. These quantities can be computed with the wavefunctions given in Sec. 4.1. Here, we will

State	Electronic energy $\varepsilon^{m\,n_\lambda n_\mu}$ of H_2^+ like systems			
$(m\,n_\mu n_\lambda)$	Equidistant grid	Exponential grid	Ref. [14]	Ref. [18]
$1s\sigma_g(000)$	**−1.102634**3945	**−1.10263421444**924	−1.102634214497	−1.1026342144949
$2s\sigma_g(001)$	**−0.3608649**972	**−0.360864875**3525	−0.36086487543	−0.3608648753383
$2p\sigma_u(010)$	**−0.6675342**981	**−0.667534392203**8	−0.667534392205	−0.6675343922024
$2p\pi_u(100)$	**−0.4287718199**	**−0.428771819888**96	−0.428771819894	−0.4287718198959
	Electronic energy $\varepsilon^{m\,n_\lambda n_\mu}$ of $\bar{p}He^+$ like systems			
	Equidistant grid	Exponential grid	Ref. [15]	
1σ (000)	**−1.5093**60191	**−1.509358482**5005	−1.5093585	
2σ (001)	**−0.250532**049	**−0.250532870**0733	−0.2505329	
3σ (010)	**−0.111359**353	**−0.1113598**082090	−0.1113598	
1π (100)	**−0.185928737**	**−0.185928739**9848	−0.1859287	

Table 2: Energies of the ground and the first few excited electronic states of H_2^+ and $\bar{p}He^+$-like systems at $R = 2$ a.u. In the first column, in brackets are shown the quantum numbers of the electronic state as defined in Eq. (7). In the second and third columns are presented our results obtained with equidistant and non-equidistant grids respectively. The reliable digits estimated by our code are in boldface. Values for the electronic energies from similar calculations by other authors are given in the last columns. The quantities in the table are in atomic units.

show the results for the molecular quadrupole moment of H_2^+ and $\bar{p}He^+$. In Cartesian coordinates, it can be found by calculating the matrix element:

$$Q(R) = \langle\phi(\mathbf{r};R)|(3z^2 - r^2)/2|\phi(\mathbf{r};R)\rangle, \tag{12}$$

where z is the projection of $\mathbf{r}$ onto the molecular axis. In spheroidal coordinates, the molecular quadrupole moment for a particular state $(m\,n_\mu n_\lambda)$ becomes:

$$\begin{aligned} Q^{m\,n_\mu n_\lambda}(R) = {} & 3R^2/8\langle\phi^{m\,n_\mu n_\lambda}(\mu,\lambda;R)|(\mu\lambda)^2|\phi^{m\,n_\mu n_\lambda}(\mu,\lambda;R)\rangle \\ & - R^2/8\langle\phi^{m\,n_\mu n_\lambda}(\mu,\lambda;R)|\mu^2+\lambda^2-1|\phi^{m\,n_\mu n_\lambda}(\mu,\lambda;R)\rangle \end{aligned} \tag{13}$$

The normalization condition of $\phi^{m\,n_\mu n_\lambda}(\mu,\lambda;R)$ is shown in Eq. (10). In Table 3, we have presented results of the R-dependent molecular quadrupole moment for the ground and a few low-excited electronic states of H_2^+ and $\bar{p}He^+$. For each state we have tabulated 15 values of $Q^{m\,n_\mu n_\lambda}(R)$ where $0.1 \le R(a.u.) \le 10$. For H_2^+ and $R = 2$, our computations are compared with the results from Ref [14]. As can be seen, a very good agreement is achieved.

In the numerical calculations of $Q(R)$, about one digit of accuracy is lost in comparison to the electronic wavefunctions' precision. As a result, the estimated precision of the calculated quadrupole moments, depending on the molecular system and its state, vary from $10 \div 11$ digits for $0.5 \le R \le 3$ to $7 \div 8$ digits for very small or very large internuclear distances.

4.3 Nonrelativistic energy spectra

The obtained in Sec. 4.1 electronic terms of three-particle systems are used to compute the nonrelativistic spectra of H_2^+ and $\bar{p}He^+$ in the Born-Oppenheimer approximation (BO). The nonrel-

R	$Q^{m\,n_\lambda n_\mu}$(R) of H_2^+			$Q^{m\,n_\lambda n_\mu}$(R) of $\bar{p}He^+$	
	$1s\sigma_g(000)$	$2s\sigma_g(001)$	$2p\sigma_u(010)$	1σ (000)	2σ (001)
0.1	0.0008367042	0.0016729471	2.9921069264	0.0150617195	0.2038915377
0.5	0.0220822318	0.0438627801	2.8136553387	0.1846148343	2.7925101281
1.0	0.0967244126	0.1886564004	2.4286797010	0.3899161256	4.9634732556
1.5	0.2395623686	0.4554188220	2.2205711774	0.6889917118	6.2897178711
2.0	0.4693517815	0.8655712644	2.3069931075	1.1103954664	7.4530161814
	0.4693517 [14]		2.306993 [14]		
2.5	0.8077743745	1.4414107617	2.6213075970	1.6584540590	8.6596201311
3.0	1.2784707756	2.2062995497	3.1080574355	2.3339290279	9.9734988541
3.5	1.9048101670	3.1844826678	3.7424433201	3.1366276174	11.415254014
4.0	2.7064139845	4.4005719996	4.5156721016	4.0661419424	12.991232279
4.5	3.6952570928	5.8786984564	5.4259243530	5.1220826480	14.702827738
5.0	4.8730010524	7.6413427042	6.4741103998	6.3041345968	16.549691091
6.0	7.7544756923	12.093088062	8.9905597271	9.0456646993	20.645423035
7.0	11.229046315	17.846062361	12.072789244	12.289424396	25.270469523
8.0	15.193830279	24.876598437	15.717234633	16.034655668	30.418047862
9.0	19.608946132	33.041999019	19.911536981	20.280901303	36.083011041
10.0	24.474527996	42.122666454	24.640528066	25.027872581	42.261535747

Table 3: Molecular quadrupole moments $Q^{m\,n_\mu n_\lambda}(R)$ for the ground and a few low-excited electronic states $(m n_\mu n_\lambda)$ of H_2^+ and $\bar{p}He^+$, where $0.1 \leq R(a.u.) \leq 10$.

ativistic energies in atomic units $E_{\nu J}$ of the studied systems for states with vibrational and rotational quantum numbers ν and J are found in BO by solving the radial Schrödinger equation (see Eq. (3)):

$$\left\{\frac{d^2}{dR^2} + 2\tilde{M}E_{\nu J} - \frac{J(J+1)-2m}{R^2} + \frac{2\tilde{M}Z_1Z_2}{R} + 2\tilde{M}\varepsilon^{m\,n_\lambda n_\mu}(R)\right\}\chi_{\nu J}^{m n_\mu n_\lambda}(R) = 0, \qquad (14)$$

where $\tilde{M} = m_2(m_1+m_3)/(m_3(m_1+m_2))$. The electronic energy $\varepsilon^{m\,n_\lambda n_\mu}(R)$ (where the zero energy is usually set to be the one of an atom consisting of the first and third particles in state $(m n_\lambda n_\mu)$) is computed by solving Eq. (7) for up to 1000 points in the interval $0.001 \leq R \leq R_{max}$. Here R_{max} is the value of R for which $\chi_{\nu J}^{m n_\mu n_\lambda}(R_{max}) \to 0$, and it depends on the particular state that is being calculated and the parameters of the program. The Hamiltonian given in Eq. (5) has a singularity at $R = 0$, which makes it difficult for numerical calculations when $R \to 0$. For $R < 0.001$ the precision of the numerical solution gradually decreases. However, for very small intermolecular distances, for the electronic terms we have used approximate formulae that give results with good accuracy (see for example Ref. [19]).

The nonrelativistic energies of H_2^+ and $\bar{p}He^+$ are computed in the Born-Oppenheimer approximation by the finite difference method with a non-equidistant grid. A few examples are shown in Table 4. In the case of the hydrogen molecular ion, both low-excited and intermediate-lying states are given. It can be seen that the number of significant digits in this basic approximation practically

System	State (ν, J)	$E, a.u.$ (BO)	Refs. [6, 11]
H_2^+	(0,0)	**−0.597**100	−0.59713906307939
	(3,4)	**−0.566**66	−0.56668823662971
	(4,1)	**−0.560**379	−0.56039717140029
$\bar{p}He^+$	(2,37)	**−2.681**50	−2.68139411
	(0,36)	**−2.886**75	−2.88668236
	(3,36)	**−2.692**67	−2.69262479

Table 4: Nonrelativistic energies in atomic units of H_2^+ and $\bar{p}He^+$ in the Born-Oppenheimer approximation. In the third column, the significant digits are in boldface.

does not change for different quantum numbers ν and J. As antiprotonic helium is normally created in highly excited states ($35 \leq J \leq 38$), those are the most important ones to be studied. Some of them are included in Table 4. The comparison with the nonrelativistic energies obtained by precise variational calculations [6, 11] reveals that the first four to five significant digits match. The precision of these results is limited from BO, as the terms corresponding to the description of the simultaneous motion of both heavy and light particles are ignored. However, it could be significantly improved by adding adiabatic corrections, as suggested in Ref. [19].

5. Conclusion

The light three-particle systems possess a number of unique characteristics that can be applied in many areas of contemporary physics: in specifying the values of fundamental constants, for the development of new time standards and quantum memories, etc. In this work, we have presented a straightforward and easy-to-implement two-dimensional finite difference method for solving the time independent Schrödinger equation on equidistant and exponential grids. Precise electronic wavefunctions for a few low-excited states of H_2^+ and $\bar{p}He^+$-like systems were obtained by this method. A comparison with existing results in the literature shows the reliability and efficiency of our code. The computed electronic terms and wavefunctions allow for fast and accurate calculations of molecule electric multipole moments. Here, we have studied the quadrupole moments of the hydrogen molecular ion and the antiprotonic helium. Examples for the ground-electronic state and a few low-excited states are presented in the work. The nonrelativistic energies of the three-particle systems have been computed in the Born-Oppenheimer approximation. A further development could be to calculate more precise nonrelativistic energy spectra in the adiabatic approach by using the obtained electronic wavefunctions. For systems consisting of one light and two heavy particles, this gives a practical alternative to the widely used variational calculations.

Acknowledgments

This work was supported by the Bulgarian Science Fund under contract KP-06-M58/3 / 22.11.2021.

References

[1] H. J. Williams *et al.*, *Magnetic Trapping and Coherent Control of Laser-Cooled Molecules*, Phys. Rev. Lett. 120, 163201 (2018).

[2] I.V. Kortunov et. al., *Proton–electron mass ratio by high-resolution optical spectroscopy of ion ensembles in the resolved-carrier regime*, Nature Physics 17, 569–573 (2021).

[3] N. Bezginov et al., *A measurement of the atomic hydrogen Lamb shift and the proton charge radius*, Science, 365, 6457 (2019).

[4] VI Korobov, D Bakalov, HJ Monkhorst, *Variational expansion for antiprotonic helium atoms*, Phys. Rev. A, (1999).

[5] S.I. Vinitskij, L.I. Ponomarev, *Adiabatic representation of three-body problem with the Coulomb interaction*, J. Phys. B. (1978).

[6] V.I. Korobov, *Variational calculation of energy levels in $\bar{p}He^+$ molecular systems*, Phys. Rev. A, 54, 3 (1996).

[7] P. Danev, D. Bakalov, V.I. Korobov, S. Schiller, *Hyperfine structure and electric quadrupole transitions in the deuterium molecular ion*, Phys. Rev. A 103 (1), 012805 (2021).

[8] A. M. Frolov & D. M. Wardlaw, *Bound state spectra of three-body muonic molecular ions*, EPJ D, 63, 339–350 (2011)

[9] Pizzolotto, C. Sbrizzi, A., Adamczak, A., Bakalov, D. *et al., Measurement of the muon transfer rate from muonic hydrogen to oxygen in the range 70-336 K, Physics Letters A, Vol. 403 (2021).*

[10] The ALPHA Collaboration, *Investigation of the fine structure of antihydrogen*, Nature, 578, 375–380 (2020).

[11] VI Korobov, *Leading-order relativistic and radiative corrections to the rovibrational spectrum of H2+ and HD+ molecular ions*, Physical Review A 74 (5), 052506 (2006).

[12] S. Schiller, D. Bakalov, and V.I. Korobov, *Simplest Molecules as Candidates for Precise Optical Clocks*, Phys. Rev. Lett. **113**, 023004 (2014).

[13] G. Hunter, B. F. Gray, and H. O. Pritchard, *Born—Oppenheimer Separation for ThreeParticle Systems. I. Theory*, J. Chem. Phys., 45, 3806 (1966).

[14] L. Laaksonen,P. Pyykkö, D. Sundholm, *Two-dimensional fully numerical solutions of molecular Schrödinger equations. I. One-electron molecules*, Int. J. Quantum Chem.y, 23, 309 - 317 (2004).

[15] I. Shimamura, *Moleculelike metastable states of antiprotonic and mesic helium*, Phys.Rev A, 47, 7 (1992).

[16] D. Hunter, K. Bates, K. Ledsham, and A. L. Stewart, *Wave functions of the hydrogen molecular ion*, Philos. Trans. R. Soc. London, Ser. A 246, 215 (1953).

[17] D. G. A. Smith, L. A. Burns, *et al.*, *Psi4 1.4: Open-Source Software for High-Throughput Quantum Chemistry*, J. Chem. Phys. (2020). (doi: 10.1063/5.0006002).

[18] M. M. Madsen and J. M. Peek, *Eigenparameters for the Lowest Twenty Electronic States of the Hydrogen Molecule Ion*, At. Data 2, 171 (1971).

[19] L. Ponomarev, T. Puzynina and N. Truskova *et al.*, *Effective potentials of the three-body problem in the adiabatic representation*, J. Phys. B: Atom. Mol. Phys. 11 3861 (1978).